Prediction of $N\Omega$-like dibaryons with heavy quarks

Hongxia Huang,[1] Jialun Ping,[1,*] and Fan Wang[2]

[1]*Department of Physics, Nanjing Normal University, Nanjing 210097, People's Republic of China*

[2]*Department of Physics, Nanjing University, Nanjing 210093, People's Republic of China*

(Received 14 November 2019; published 13 January 2020)

Possible $N\Omega$-like dibaryons $N\Omega_{ccc}$ and $N\Omega_{bbb}$ are investigated within the framework of two quark models: the chiral quark model (ChQM) and quark delocalization color screening model (QDCSM). We find both of these two states are bound in these two models, and the binding energy increases as the quark of the system becomes heavier. In the ChQM, only coupling both color-singlet and hidden-color channels can make the $N\Omega_{ccc}$ and $N\Omega_{bbb}$ systems bound. While in the QDCSM, the attraction between N and Ω_{ccc} (or Ω_{bbb}) mainly comes from the kinetic energy term due to quark delocalization and color screening. The effect of channel coupling provides more effective attraction to $N\Omega_{ccc}$ and $N\Omega_{bbb}$ systems. Besides, the calculation of the low-energy scattering phase shifts, the scattering length, the effective range, and the binding energy (obtained from the scattering length) also supports the existence of the $N\Omega_{ccc}$ and $N\Omega_{bbb}$ states. All these properties can provide more information for experimental search for the $N\Omega$-like dibaryons with heavy quarks. And the experimental progress can also check the mechanism of the intermediate-range attraction of the baryon-baryon interaction in quark models.

DOI: 10.1103/PhysRevC.101.015204

I. INTRODUCTION

The study of dibaryons is one of the long-standing problems in hadron physics. Although research on the dibaryon has experienced several ups and downs in its long history, dibaryons have received renewed interest in recent years. For the nonstrange dibaryon, the best-known candidate is the $\Delta\Delta$ resonance state, which was predicted by Dyson and Xuong in 1964 [1] and later also by Goldman *et al.*, who called it the "inevitable dibaryon" d^* due to its unique symmetry features [2]. Recently, the WASA-at-COSY collaboration reported the discovery of this $\Delta\Delta$ resonance state with $M = 2.37$ GeV, $\Gamma \approx 70$ MeV, and $IJ^P = 03^+$ [3–5]. The detail of this dibaryon observation can be found in Ref. [6]. The quark model calculations [7–10], as well as the relativistic three-body calculations [11,12] all described properly the characteristics of this resonance.

For the strange dibaryon, the H-dibaryon with $J = 0$, $S = -2$, the $N\Omega$ with $J = 2$, $S = -3$, and the $\Omega\Omega$ with $J = 0$, $S = -6$ are particularly interesting, since the Pauli blocking among valence quarks do not operate in these systems. Above all, the progress of the $N\Omega$ searches in experiment attracted more and more attention for this state. Very recently, the measurement of the $p\Omega$ correlation function was conducted in Au + Au collisions by the STAR experiment at the Relativistic Heavy Ion Collider (RHIC) [13], and the result indicated that the scattering length is positive for the $p\Omega$ interaction and favored the $p\Omega$ bound-state hypothesis. On the theoretical side, the $N\Omega$ state has been investigated by several groups. Goldman *et al.* predicted that the $S = -3$, $I = 1/2$, $J = 2$ dibaryon state $N\Omega$ might be a narrow resonance in a relativistic quark model [14]. Oka proposed that there should be a quasibound state with $IJ^P = \frac{1}{2}2^+$ by using a constituent quark model [15]. Recent study of (2 + 1)-flavor lattice quantum chromodynamics (QCD) simulations by HAL QCD Collaboration reported that the $N\Omega$ was indeed a bound state at pion mass of 875 MeV [16] and later with nearly physical quark masses ($m_\pi \simeq 146$ MeV and $m_K \simeq 525$ MeV) [17]. K. Morita *et al.* studied the two-pair momentum correlation functions of the dibaryon candidate $N\Omega$ in relativistic heavy-ion collisions by employing the interactions obtained from the (2 + 1)-flavor lattice QCD simulations [18,19]. Besides, this state has also been observed to be bound in several relativistic quark models [20–24].

For the dibaryons with heavy quarks, the $N\Lambda_c$ system and the H-like dibaryon state $\Lambda_c\Lambda_c$ were both studied on the hadron level [25,26] and on the quark level [27,28]. The possibility of existing deuteron-like dibaryons with heavy quarks, such as $N\Sigma_c$, $N\Xi_c'$, $N\Xi_{cc}$, $\Xi\Xi_{cc}$, and so on, were investigated by several realistic phenomenological nucleon-nucleon interaction models [29,30]. Recently many near-threshold charmonium-like states called XYZ particles were observed, triggering many studies on the molecule-like bound states containing heavy-quark hadrons. Such studies will give further information on the hadron-hadron interactions. In the heavy-quark sector, the large masses of the heavy quarks reduce the kinetic energy of the

*Corresponding author: jlping@njnu.edu.cn

system, which makes them easier to form bound states. Very recently, the lattice QCD also studied the deuteron-like dibaryons with heavy quarks, which include valence quark contents: $\Sigma_c\Xi_{cc}(uucucc)$, $\Omega_c\Omega_{cc}(sscscc)$, $\Sigma_b\Xi_{bb}(uububb)$, $\Omega_b\Omega_{bb}(ssbsbb)$, and $\Omega_{ccb}\Omega_{cbb}(ccbcbb)$ and with spin-parity $J^P = 1^+$ [31]. They also found that the binding of these dibaryons became stronger as they became heavier in mass. Therefore, the dibaryons with heavy quarks are also possible multiquark states, and the study of such system will help us to understand the hadron-hadron interactions and search for exotic quark states in temporary hadron physics.

It is known to all that QCD is the fundamental theory of the strong interaction in the perturbative region. However, in the low-energy region, it is difficult to directly use QCD to study complicated systems such as hadron-hadron interactions and multiquark states because of the nonperturbative complication. Various QCD-inspired models have been developed to get physical insights into the multiquark systems. The quark delocalization color screening model (QDCSM), developed in the 1990s with the aim of explaining the similarities between nuclear and molecular forces [32], is one of the representations of the quark models. In this model, quarks confined in one nucleon are allowed to delocalize to a nearby baryon and the confinement interaction between quarks in different baryon orbits is modified to include a color screening factor. The latter is a model description of the hidden-color-channel coupling effect [33]. The delocalization parameter is determined by the dynamics of the interacting quark system; this allows the quark system to choose the most favorable configuration through its own dynamics in a larger Hilbert space. The model gives a good description of NN and YN interactions and the properties of deuteron [34,35]. It is also employed to study the dibaryon candidates d^* [7,8] and $N\Omega$ [20–23] and dibaryons with heavy quarks, the $N\Lambda_c$ system and the $\Lambda_c\Lambda_c$ system [27,28].

Another commonly used quark model is the chiral quark model (ChQM) [36,37], in which the constituent quarks interact with each other through colorless Goldstone boson exchange in addition to the colorful one-gluon exchange and color confinement. In this model, the chiral partner σ meson exchange is introduced to obtain the immediate-range attraction of NN interaction. We have shown that the NN intermediate-range attraction mechanism in the QDCSM, quark delocalization and color screening, is equivalent to σ meson exchange in the ChQM [35]. When extending to the $N\Omega$ system [23], the ChQM only has Goldstone boson exchange, since the σ meson should not exchange between $u(d)$ and s quark. The ChQM can accommodate a bound $N\Omega$ state only if both the color-singlet and hidden-color-channels coupling is considered. On the other hand, the QDCSM predicts there will be a bound $N\Omega$ state with only color-singlet-channels coupling. This indicates that the quark delocalization and color screening with the five-color-singlet-channels coupling provides enough effective attraction to bound the $N\Omega$ system.

In this work, we continue to investigate dibaryons with heavy quarks by using these two models. In our previous work, we have shown $N\Omega$ is a narrow resonance in the $\Lambda\Xi$ D-wave scattering process [22]. However, Λ-Ξ scattering data analysis is quite complicated. Then we calculated the low-energy $N\Omega$ scattering phase shifts, scattering length, effective range, and binding energy, which can be observed by the N-Ω correlation analysis with RHIC and large hadron collider (LHC) data or by the new developed automatic scanning system at Japan proton accelerator research complex (J-PARC) [23]. It is interesting to extend such study to the dibaryons on heavy quark sector. So we investigate whether the $N\Omega$-like dibaryons $N\Omega_{ccc}$ and $N\Omega_{bbb}$ exist or not in quark models. The low-energy scattering phase shifts, scattering length, effective range, and binding energy of $N\Omega_{ccc}$ and $N\Omega_{bbb}$ may also be useful for the experimental search of such heavy dibaryons. Besides, by comparing the results within two quark models, we can check the model dependence of the dibaryons prediction.

The structure of this paper is as follows. A brief introduction of two quark models is given in Sec. II. Section III devotes to the numerical results and discussions. The summary is shown in the last section.

II. TWO QUARK MODELS

As mentioned above, we use two quark models, the ChQM and QDCSM, to study $N\Omega$-like dibaryons with heavy quarks.

A. Chiral quark model

The chiral quark model can give a good description of the hadron spectra, nucleon-nucleon interaction, and multiquark states. In this model, the constituent quarks interact with each other through Goldstone boson exchange and one-gluon exchange in addition to color confinement. The model details can be found in Ref. [37]. Here we only give the Hamiltonian:

$$H = \sum_{i=1}^{6}\left(m_i + \frac{p_i^2}{2m_i}\right) - T_{\mathrm{c.m.}} + \sum_{j>i=1}^{6}\left(V_{ij}^C + V_{ij}^G + V_{ij}^\chi + V_{ij}^\sigma\right), \tag{1}$$

$$V_{ij}^C = -a_c\boldsymbol{\lambda}_i^c\cdot\boldsymbol{\lambda}_j^c\left(r_{ij}^2 + v_0\right), \tag{2}$$

$$V_{ij}^G = \frac{1}{4}\alpha_s\boldsymbol{\lambda}_i^c\cdot\boldsymbol{\lambda}_j^c\left[\frac{1}{r_{ij}} - \frac{\pi}{2}\delta(\boldsymbol{r}_{ij})\left(\frac{1}{m_i^2} + \frac{1}{m_j^2} + \frac{4\boldsymbol{\sigma}_i\cdot\boldsymbol{\sigma}_j}{3m_im_j}\right) - \frac{3}{4m_im_jr_{ij}^3}S_{ij}\right], \tag{3}$$

$$V_{ij}^\chi = V_\pi(\boldsymbol{r}_{ij})\sum_{a=1}^{3}\lambda_i^a\cdot\lambda_j^a + V_K(\boldsymbol{r}_{ij})\sum_{a=4}^{7}\lambda_i^a\cdot\lambda_j^a + V_\eta(\boldsymbol{r}_{ij})\left[\left(\lambda_i^8\cdot\lambda_j^8\right)\cos\theta_P - \left(\lambda_i^0\cdot\lambda_j^0\right)\sin\theta_P\right] \tag{4}$$

$$V_\chi(\boldsymbol{r}_{ij}) = \frac{g_{\rm ch}^2}{4\pi}\frac{m_\chi^2}{12m_im_j}\frac{\Lambda_\chi^2}{\Lambda_\chi^2-m_\chi^2}m_\chi\left\{(\boldsymbol{\sigma}_i\cdot\boldsymbol{\sigma}_j)\left[Y(m_\chi r_{ij})-\frac{\Lambda_\chi^3}{m_\chi^3}Y(\Lambda_\chi r_{ij})\right]+\left[H(m_\chi r_{ij})-\frac{\Lambda_\chi^3}{m_\chi^3}H(\Lambda_\chi r_{ij})\right]S_{ij}\right\}, \quad \chi=\pi, K, \eta, \tag{5}$$

$$V_{ij}^\sigma = -\frac{g_{\rm ch}^2}{4\pi}\frac{\Lambda_\sigma^2}{\Lambda_\sigma^2-m_\sigma^2}m_\sigma\left[Y(m_\sigma r_{ij})-\frac{\Lambda_\sigma}{m_\sigma}Y(\Lambda_\sigma r_{ij})\right], \tag{6}$$

$$S_{ij} = \left\{3\frac{(\boldsymbol{\sigma}_i\cdot\boldsymbol{r}_{ij})(\boldsymbol{\sigma}_j\cdot\boldsymbol{r}_{ij})}{r_{ij}^2}-\boldsymbol{\sigma}_i\cdot\boldsymbol{\sigma}_j\right\}, \tag{7}$$

$$H(x) = (1+3/x+3/x^2)Y(x), \qquad Y(x)=e^{-x}/x, \tag{8}$$

where S_{ij} is quark tensor operator; $Y(x)$ and $H(x)$ are standard Yukawa functions; $T_{\rm c.m.}$ is the kinetic energy of the center of mass; $\alpha_{\rm ch}$ is the chiral coupling constant, determined as usual from the π-nucleon coupling constant; and α_s is the quark-gluon coupling constant. In order to cover the wide energy range from light to strange to heavy quarks, an effective scale-dependent quark-gluon coupling $\alpha_s(u)$ was introduced [38]:

$$\alpha_s(u) = \frac{\alpha_0}{\ln\left(\frac{u^2+u_0^2}{\Lambda_0^2}\right)}. \tag{9}$$

The other symbols in the above expressions have their usual meanings. Here we should mention that the σ meson is restricted to exchange between the u and/or d quark pair only. The parameters are taken from our previous work [23], except the mass of heavy quarks, which are determined by fitting the masses of charm and bottom baryons.

B. The quark delocalization color screening model

The Hamiltonian of the QDCSM is almost the same as that of the ChQM, except for two modifications [32,34]. First, there is no σ-meson exchange in the QDCSM. Second, the screened color confinement is used between quark pairs reside in different baryon orbits. That is

$$V_{ij}^C = \begin{cases} -a_c\boldsymbol{\lambda}_i^c\cdot\boldsymbol{\lambda}_j^c\,(r_{ij}^2+v_0) & \text{if } i,j \text{ in the same baryon orbit} \\ -a_c\boldsymbol{\lambda}_i^c\cdot\boldsymbol{\lambda}_j^c\left(\frac{1-e^{-\mu_{ij}\mathbf{r}_{ij}^2}}{\mu_{ij}}+v_0\right) & \text{otherwise} \end{cases}. \tag{10}$$

TABLE I. Model parameters: $m_\pi = 0.7$ fm^{-1}, $m_K = 2.51$ fm^{-1}, $m_\eta = 2.77$ fm^{-1}, $m_\sigma = 3.42$ fm^{-1}, $\Lambda_\pi = 4.2$ fm^{-1}, $\Lambda_K = 5.2$ fm^{-1}, $\Lambda_\eta = 5.2$ fm^{-1}, $\Lambda_\sigma = 4.2$ fm^{-1}, $\alpha_{\rm ch} = 0.027$.

	b (fm)	$m_{u,d}$ (MeV)	m_s (MeV)	m_c (MeV)	m_b (MeV)
ChQM	0.518	313	536	1744	5100
QDCSM	0.518	313	573	1788	5141
	a_c (MeV fm^{-2})	V_0 (MeV)	α_0	Λ_0 (fm^{-1})	u_0 (MeV)
ChQM	48.59	−1.2145	0.510	1.525	445.808
QDCSM	58.03	−1.2883	0.510	1.525	445.808

All parameters, which are fixed by fitting to the masses of baryons with light flavors and heavy flavors, are taken from our previous work [28]. The values of the parameters of two models are listed in Table I. The masses of light flavor baryons are shown in our former work [23]; here we just list the masses of the charm and bottom baryons in Table II.

The quark delocalization in the QDCSM is realized by specifying the single-particle orbital wave function of the QDCSM as a linear combination of left and right Gaussians, the single-particle orbital wave functions used in the ordinary quark cluster model,

$$\begin{aligned} \psi_\alpha(\mathbf{s}_i,\epsilon) &= [\phi_\alpha(\mathbf{s}_i)+\epsilon\phi_\alpha(-\mathbf{s}_i)]/N(\epsilon), \\ \psi_\beta(-\mathbf{s}_i,\epsilon) &= [\phi_\beta(-\mathbf{s}_i)+\epsilon\phi_\beta(\mathbf{s}_i)]/N(\epsilon), \\ N(\epsilon) &= \sqrt{1+\epsilon^2+2\epsilon e^{-s_i^2/4b^2}}. \\ \phi_\alpha(\mathbf{s}_i) &= \left(\frac{1}{\pi b^2}\right)^{3/4} e^{-\frac{1}{2b^2}(\mathbf{r}_\alpha-\mathbf{s}_i/2)^2} \\ \phi_\beta(-\mathbf{s}_i) &= \left(\frac{1}{\pi b^2}\right)^{3/4} e^{-\frac{1}{2b^2}(\mathbf{r}_\beta+\mathbf{s}_i/2)^2}. \end{aligned} \tag{11}$$

Here $\mathbf{s}_i$, $i = 1, 2, \ldots, n$ are the generating coordinates, which are introduced to expand the relative motion wave function. The delocalization parameter $\epsilon(\mathbf{s}_i)$ is determined by the dynamics of the quark system rather than adjusted parameters. In this way, the system can choose its most favorable configuration through its own dynamics in a larger Hilbert space. It has been used to explain the crossover transition between hadron phase and quark-gluon plasma phase [40].

TABLE II. The masses (in MeV) of the charmed and bottom baryons. Experimental values are taken from the Particle Data Group (PDG) [39].

	Σ_c	Σ_c^*	Λ_c	Ξ_c	Ξ_c^*	Ξ_{cc}	Ξ_{cc}^*	Ω_c	Ω_{ccc}
Expt.	2455	2520	2286	2467	2645	3621	—	2695	—
ChQM	2465	2490	2286	2537	2631	3744	3770	2746	5069
QDCSM	2465	2489	2286	2551	2638	3766	3792	2786	5135
	Σ_b	Σ_b^*	Λ_b	Ξ_b	Ξ_b^*	Ξ_{bb}	Ξ_{bb}^*	Ω_b	Ω_{bbb}
Expt.	5811	5832	5619	5792	5955	—	—	6046	—
ChQM	5811	5820	5622	5877	5966	10438	10447	6094	15112
QDCSM	5809	5817	5619	5888	5971	10455	10464	6131	15169

TABLE III. Channels of the $N\Omega_{ccc}$ system.

1	2	3	4	5	6	7	8
$\Xi^*_{cc}\Sigma_c$	$\Xi_{cc}\Sigma^*_c$	$\Xi^*_{cc}\Lambda_c$	$N\Omega_{ccc}$	$\Xi^*_{cc}\Sigma^*_c$	$\Xi''_{cc}\Sigma^{*\prime}_c$	$\Xi^{*\prime}_{cc}\Sigma''_c$	$\Xi''_{cc}\Sigma''_c$
9	10	11	12	13	14	15	16
$\Xi''\Sigma$	$N'\Omega'_{ccc}$	$\Xi^{*\prime}_{cc}\Lambda''_c$	$\Xi'_{cc}\Lambda''_c$	$\Xi''_{cc}\Lambda''_c$	$\Xi''_{cc}\Lambda'''_c$	$\Xi'_{cc}\Sigma''_c$	$\Xi''_{cc}\Lambda'_c$

III. THE RESULTS AND DISCUSSIONS

In this work, we investigate the $N\Omega$-like dibaryons with heavy quarks: $N\Omega_{ccc}$ and $N\Omega_{bbb}$ systems with quantum numbers $IJ^P = \frac{1}{2}2^+$ in two quark models: the ChQM and QDCSM. The effects of channel coupling are studied here, both color-singlet channels (the color symmetry of the $3q$ cluster is [111]) and hidden-color channels (the color symmetry of the $3q$ cluster is [21]) are included. The labels of the hidden-color $3q$ cluster can be found in Ref. [23]. Here we list all 16 coupled channels of the $N\Omega_{ccc}$ system in Table III, where the first 5 channels are color-singlet channels and the last 11 ones are hidden-color channels.

To check whether there is any bound state, a dynamical calculation is needed. The resonating group method (RGM) [41] is employed here. By expanding the relative motion wave function between two clusters in the RGM equation by Gaussians, the integro-differential equation of the RGM can be reduced to an algebraic equation, which is the generalized eigenequation. Then, by solving the eigenequation, the energy of the system can be obtained. Besides, to keep the matrix dimension manageably small, the baryon-baryon separation is taken to be less than 6 fm in the calculation.

For the $N\Omega_{ccc}$ system, the binding energies of the $N\Omega_{ccc}$ state in the ChQM and QDCSM are listed in Table IV, where $B_{\rm sc}$ denotes the binding energy of the single-channel $N\Omega_{ccc}$, B_{5cc} refers to the binding energy with 5-color-singlet-channels coupling, and B_{16cc} denotes the binding energy with all 16-channel coupling; "ub" denotes that the state is unbound. The single-channel calculation shows that the $N\Omega_{ccc}$ is unbound in the ChQM. The effect of color-singlet-channels coupling is not large enough to make the $N\Omega_{ccc}$ bound; only additional hidden-color-channels coupling leads to the bound $N\Omega_{ccc}$ state. In the QDCSM, the single-channel calculation shows that the $N\Omega_{ccc}$ is bound with very small binding energies. Since it already contains the hidden-color-channels coupling effect through color screening [33], we only include the color-singlet-channels coupling here. We find that the lowest energy of the system is 30.9 MeV lower than the threshold of $N\Omega_{ccc}$, which means that this heavy-quark dibaryon $N\Omega_{ccc}$ is a bound state in the QDCSM. Obviously, the effect of channel coupling is important for providing more effective attractions to the $N\Omega_{ccc}$ systems in the QDCSM. All these results are consistent with our previous study of $N\Omega$ system [23], in which we found that the QDCSM with color-singlet-channels coupling obtained similar results to that of the ChQM with both color-singlet and hidden-color-channels coupling.

TABLE IV. The binding energies of the $N\Omega_{ccc}$ system with channel coupling.

	$B_{\rm sc}$ (MeV)	B_{5cc} (MeV)	B_{16cc} (MeV)
ChQM	ub	ub	−16.4
QDCSM	−0.6	−30.9	...

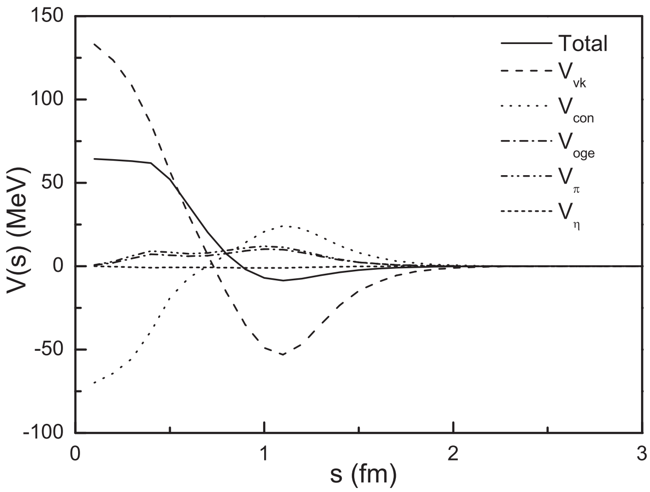

FIG. 1. The contributions to the effective potential from various terms of interactions in the QDCSM.

To understand the interaction between N and Ω_{ccc}, we study the effective potentials, as well as the contribution of each interaction term to the energy of the system. In the ChQM, the confinement, the one-gluon exchange, does not contribute to the effective potential between N and Ω_{ccc}, because there is no quark exchange between these two baryons. The π, K, η, and σ mesons do not contribute either because they do not exchange between the $u(d)$ and c quarks. There is only kinetic energy, which provide the repulsive interactions between N and Ω_{ccc}. That is why the individual $N\Omega_{ccc}$ channel is unbound in the ChQM.

Things are different in the QDCSM. The quark exchange happens between N and Ω_{ccc}, due to quark delocalization. The total effective potentials and the contributions of all interaction terms, including the kinetic energy ($V_{\rm vk}$), the confinement ($V_{\rm con}$), the one-gluon exchange ($V_{\rm oge}$), the π exchange (V_π), and the η exchange (V_η), to the effective potential are shown in Fig. 1. We notice that, due to the special quark content of $N\Omega_{ccc}$ system, the effective interactions have very small contributions from the one-gluon-exchange interaction. The attraction of the $N\Omega_{ccc}$ state mainly comes from the kinetic energy term due to quark delocalization and color screening, and other terms provide repulsive potentials, which reduce the total attraction of the $N\Omega_{ccc}$ potential. By comparing with the interaction between N and Ω [23], this behavior is similar. The intermediate-range attraction in the QDCSM comes from quark delocalization and color screening, which work together to provide short-range repulsion and intermediate-range attraction.

In our previous work, we also calculated the low-energy scattering phase shifts, scattering length, and effective range of $N\Omega$, which can provide necessary information for N-Ω correlation analysis with RHIC and LHC data. Naturally, we do the same calculation for the $N\Omega_{ccc}$ and $N\Omega_{bbb}$ systems. The low-energy scattering phase shifts are calculated by using the well-developed Kohn-Hulthen-Kato variational method [41]. The wave function of the dibaryon system is of the form

$$\Psi = \mathcal{A}\big[\hat{\phi}_A(\boldsymbol{\xi}_1, \boldsymbol{\xi}_2)\hat{\phi}_B(\boldsymbol{\xi}_3, \boldsymbol{\xi}_4)\chi_L(\boldsymbol{R}_{AB})\big], \tag{12}$$

where $\boldsymbol{\xi}_1$ and $\boldsymbol{\xi}_2$ are the internal coordinates for the baryon cluster A and $\boldsymbol{\xi}_3$ and $\boldsymbol{\xi}_4$ are the internal coordinates for another baryon cluster B. $\boldsymbol{R}_{AB} = \boldsymbol{R}_A - \boldsymbol{R}_B$ is the relative coordinate between the two clusters. The symbol $\mathcal{A}$ is the antisymmetrization operator; $\hat{\phi}_A$ and $\hat{\phi}_B$ are the internal cluster wave functions of two baryons, A and B, and $\chi_L(\boldsymbol{R}_{AB})$ is the relative motion wave function between two clusters. For a scattering problem, $\chi_L(\boldsymbol{R}_{AB})$ is expanded as

$$\chi_L(\boldsymbol{R}_{AB}) = \sum_{i=1}^{n} C_i \frac{\tilde{u}_L(R_{AB}, S_i)}{R_{AB}} Y_{LM}(\hat{\boldsymbol{R}}_{AB}) \tag{13}$$

with

$$\tilde{u}_L(R_{AB}, S_i) = \begin{cases} \alpha_i u_L(R_{AB}, S_i), & R_{AB} \leqslant R_C \\ [h_L^-(k_{AB}, R_{AB}) - s_i h_L^+(k_{AB}, R_{AB})] & R_{AB}, R_{AB} \geqslant R_C \end{cases}, \tag{14}$$

where

$$u_L(R_{AB}, S_i) = \sqrt{4\pi}\left(\frac{3}{2\pi b^2}\right)^{3/4} R_{AB} \times \exp\left[-\frac{3}{4b^2}\left(R_{AB}^2 - S_i^2\right)\right] i^L j_L\left(-i\frac{3}{2b^2}R_{AB}S_i\right), \tag{15}$$

where $\boldsymbol{S}_i$ is the generating coordinate, C_i are expansion coefficients, and n is the number of the Gaussian bases, which is determined by the stability of the results. In addition, $h_L^{\pm}$ are the Lth spherical Hankel functions, k_{AB} is the momentum of relative motion with $k_{AB} = \sqrt{2\mu_{AB}E_{\text{c.m.}}}$, μ_{AB} is the reduced mass of two hadrons (A and B) of the open channel, $E_{\text{c.m.}}$ is the incident energy, and R_C is a cutoff radius beyond which all the strong interaction can be disregarded. Also, α_i and s_i are complex parameters which are determined by the smoothness condition at $R_{AB} = R_C$ and C_i satisfy $\sum_{i=1}^{n} C_i = 1$; j_L is the Lth spherical Bessel function. After performing variational procedure, a Lth partial-wave equation for the scattering problem can be deduced as

$$\sum_{j=1}^{n} \mathcal{L}_{ij}^L C_j = \mathcal{M}_i^L \quad (i = 0, 1, \ldots, n-1), \tag{16}$$

with

$$\mathcal{L}_{ij}^L = \mathcal{K}_{ij}^L - \mathcal{K}_{i0}^L - \mathcal{K}_{0j}^L + \mathcal{K}_{00}^L, \tag{17}$$

$$\mathcal{M}_i^L = \mathcal{K}_{00}^L - \mathcal{K}_{i0}^L, \tag{18}$$

and

$$\mathcal{K}_{ij}^L = \left\langle \hat{\phi}_A(\boldsymbol{\xi}_1', \boldsymbol{\xi}_2')\hat{\phi}_B(\boldsymbol{\xi}_3', \boldsymbol{\xi}_4')\frac{\tilde{u}_L(R_{AB}', S_i)}{R_{AB}'} Y_{LM}(\hat{\boldsymbol{R}}_{AB}') \right. |H - E| \left. \mathcal{A}\left[\hat{\phi}_A(\boldsymbol{\xi}_1, \boldsymbol{\xi}_2)\hat{\phi}_B(\boldsymbol{\xi}_3, \boldsymbol{\xi}_4)\frac{\tilde{u}_L(R_{AB}, S_j)}{R_{AB}} Y_{LM}(\hat{\boldsymbol{R}}_{AB})\right]\right\rangle. \tag{19}$$

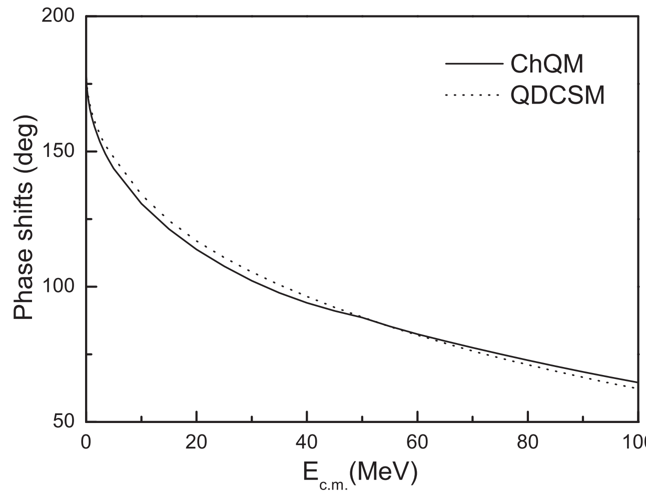

FIG. 2. The phase shifts of the $N\Omega_{ccc}$ state in both the ChQM and QDCSM.

By solving Eq. (16), we can obtain the expansion coefficients C_i. Then the scattering matrix element S_L and the phase shifts δ_L are given by

$$S_L \equiv e^{2i\delta_L} = \sum_{i=1}^{n} C_i s_i. \tag{20}$$

Then we can extract the scattering length a_0 and the effective range r_0 from the low-energy phase shifts by using the formula:

$$k_{AB}\cot\delta_L = -\frac{1}{a_0} + \frac{1}{2}r_0 k_{AB}^2 + \mathcal{O}\left(k_{AB}^4\right). \tag{21}$$

Finally, the binding energy B' is calculated according to the relation:

$$B' = \frac{\hbar^2\alpha^2}{2\mu_{AB}}, \tag{22}$$

where α is the wave number which can be obtained from the relation [42]:

$$r_0 = \frac{2}{\alpha}\left(1 - \frac{1}{\alpha a_0}\right). \tag{23}$$

Please note that by using the low-energy phase shifts, the binding energy can also be estimated. Here we label it as B'. The low-energy phase shifts are shown in Fig. 2, and the scattering length, the effective range, as well as the binding energy B' are listed in Table V. All results are calculated with

TABLE V. The scattering length a_0, effective range r_0, and binding energy B' of the $N\Omega_{ccc}$ state.

	a_0 (fm)	r_0 (fm)	B' (MeV)
ChQM	1.4989	0.40810	−15.5
QDCSM	1.3347	0.43343	−21.6

TABLE VI. The binding energies of the $N\Omega_{bbb}$ system with channel coupling.

	B_{sc} (MeV)	B_{5cc} (MeV)	B_{16cc} (MeV)
ChQM	ub	ub	−16.4
QDCSM	ub	−50.7	—

5-channel coupling in the QDCSM and 16-channel coupling in the ChQM.

It is obvious that the scattering phase shifts of the $N\Omega_{ccc}$ state in both the ChQM and QDCSM go to π at $E_{\mathrm{c.m.}} \sim 0$ and rapidly decreases as $E_{\mathrm{c.m.}}$ increases, which implies the existence of the bound $N\Omega_{ccc}$ state. The pattern of the phase shifts in the low-energy region is similar to that of the $N\Omega$ state [23]. From Table V, we can see that the scattering length of the $N\Omega_{ccc}$ state in both the ChQM and QDCSM are all positive, which implies again that this state is a bound state. The binding energy B' of this state is close to the binding energy B obtained in the bound-state calculations shown above. It indicates that the binding energy from the two methods are coincident with each other.

Particularly, we also extend the study to the $N\Omega_{bbb}$ system because of the heavy flavor symmetry. The numerical results are listed in Table VI and Table VII. The phase shifts of the $N\Omega_{bbb}$ state in both the ChQM and QDCSM are shown in Fig. 3. The results are similar to the $N\Omega_{ccc}$ system. The $N\Omega_{bbb}$ state is bound in the ChQM by coupling all color-singlet and hidden-color channels, and it is also bound in the QDCSM with color-singlet-channels coupling only. The low-energy phase shifts, the scattering length, the effective range, as well as the binding energy B' also favor the existence of the $N\Omega_{bbb}$ bound state. Besides, by comparing with the dibaryon $N\Omega$ [23] and $N\Omega_{ccc}$, we find that the binding energy increases as the quark of the system becomes heavier. This conclusion is consistent with the recent work of lattice QCD [31], in which they studied the deuteron-like dibaryons with heavy quarks and found that the stability of dibaryons increases as they become heavier.

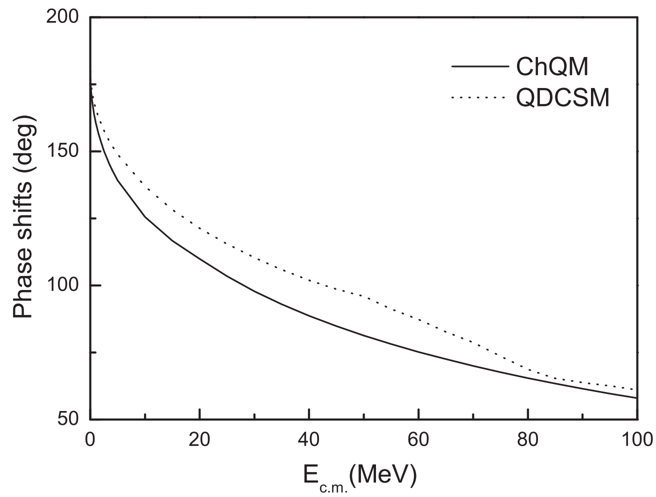

FIG. 3. The phase shifts of the $N\Omega_{bbb}$ state in both the ChQM and QDCSM.

IV. SUMMARY

In this work, we investigate the $N\Omega$-like dibaryons with heavy quarks: $N\Omega_{ccc}$ and $N\Omega_{bbb}$ systems with quantum numbers $IJ^P = \frac{1}{2}2^+$ in the framework of two quark models: the ChQM and QDCSM. Our results show that both of these two states are bound in two models. However, the factors leading to such bound states are different. In the ChQM, the confinement, one-gluon exchange, as well as the π, K, η, and σ mesons, do not contribute to the effective potential between N and Ω_{ccc} (or Ω_{bbb}), due to the special quark content of $N\Omega_{ccc}$ and $N\Omega_{bbb}$ systems. Only coupling all color-singlet and hidden-color channels can make the $N\Omega_{ccc}$ and $N\Omega_{bbb}$ systems bound. Whereas in the QDCSM, the attraction between N and Ω_{ccc} (or Ω_{bbb}) mainly comes from the kinetic energy term due to quark delocalization and color screening. Besides, the channel coupling of color-singlet channels also plays an important role for providing more effective attraction to the $N\Omega_{ccc}$ and $N\Omega_{bbb}$ systems. This behavior of these two states is similar to that of the $N\Omega$ system. The study of the $N\Omega$ system, as well as the $N\Omega_{ccc}$ and $N\Omega_{bbb}$ systems, opens a new window to investigate the hadron-hadron interaction. Considerable headway in the search for the $N\Omega$ bound state was made by the STAR experiment. If the existence of the $N\Omega$ state can be confirmed by experiments, it will be a signal showing that the mechanism of quark delocalization and color screening is really responsible for the intermediate-range attraction of the baryon-baryon interaction.

By comparing the results of the $N\Omega$, $N\Omega_{ccc}$, and $N\Omega_{bbb}$ states, we find that the binding of these dibaryons becomes stronger as they become heavier, which indicates that it is more possible for the $N\Omega_{ccc}$ and $N\Omega_{bbb}$ states to be bound. So it is worth looking for such $N\Omega$-like dibaryons in the experiments, although it will be a challenging subject because of their low production yields. It is expected that the calculated the low-energy scattering phase shifts (the scattering length, the effective range, and the binding energy) are beneficial to the experimental search for $N\Omega$-like dibaryons in the two-baryon correlation analysis approach.

TABLE VII. The scattering length a_0, effective range r_0, and binding energy B' of the $N\Omega_{bbb}$ state.

	a_0 (fm)	r_0 (fm)	B' (MeV)
ChQM	1.5981	0.66427	−40.1
QDCSM	1.1608	0.53617	−40.1

ACKNOWLEDGMENTS

This work is supported partly by the National Natural Science Foundation of China under Contracts No. 11675080, No. 11775118, and No. 11535005.

[1] F. J. Dyson and N. H. Xuong, Phys. Rev. Lett. **13**, 815 (1964).
[2] T. Goldman, K. Maltman, G. J. Stephenson, K. E. Schmidt, and F. Wang, Phys. Rev. C **39**, 1889 (1989).
[3] M. Bashkanov, C. Bargholtz, M. Berlowski, D. Bogoslawsky, H. Calen, H. Clement, L. Demiroers, E. Doroshkevich, D. Duniec, C. Ekstrom, K. Fransson, L. Geren, L. Gustafsson, B. Hoistad, G. Ivanov, M. Jacewicz, E. Jiganov, T. Johansson, O. Khakimova, S. Keleta, I. Koch, F. Kren, S. Kullander, A. Kupsc, K. Lindberg, P. Marciniewski, R. Meier, B. Morosov, C. Pauly, H. Pettersson, Y. Petukhov, A. Povtorejko, A. Pricking, R. J. M. Y. Ruber, K. Schonning, W. Scobel, B. Shwartz, T. Skorodko, V. Sopov, J. Stepaniak, P. E. Tegner, P. Thorngren-Engblom, V. Tikhomirov, A. Turowiecki, G. J. Wagner, M. Wolke, J. Zabierowski, I. Zartova, and J. Zlomanczuk (CELSIUS/WASA Collaboration), Phys. Rev. Lett. **102**, 052301 (2009).
[4] P. Adlarson *et al.* (WASA-at-COSY Collaboration), Phys. Rev. Lett. **106**, 242302 (2011).
[5] P. Adlarson *et al.* (WASA-at-COSY Collaboration), Phys. Rev. Lett. **112**, 202301 (2014).
[6] H. Clement, Progr. Part. Nucl. Phys. **93**, 195 (2017).
[7] J. L. Ping, H. X. Huang, H. R. Pang, F. Wang, and C. W. Wong, Phys. Rev. C **79**, 024001 (2009).
[8] H. Huang, J. Ping, and F. Wang, Phys. Rev. C **89**, 034001 (2014).
[9] X. Q. Yuan, Z. Y. Zhang, Y. W. Yu, and P. N. Shen, Phys. Rev. C **60**, 045203 (1999).
[10] F. Huang, Z. Y. Zhang, P. N. Shen, and W. L. Wang, Chin. Phys. C **39**, 071001 (2015).
[11] A. Gal and H. Garcilazo, Phys. Rev. Lett. **111**, 172301 (2013).
[12] A. Gal and H. Garcilazo, Nucl. Phys. A **928**, 73 (2014).
[13] J. Adam *et al.* (STAR Collaboration), Phys. Lett. B **790**, 490 (2019).
[14] T. Goldman, K. Maltman, G. J. Stephenson, K. E. Schmidt, and F. Wang, Phys. Rev. Lett. **59**, 627 (1987).
[15] M. Oka, Phys. Rev. D **38**, 298 (1988).
[16] F. Etminan *et al.* (HAL QCD Collaboration), Nucl. Phys. A **928**, 89 (2014).
[17] T. Iritani *et al.* (HAL QCD Collaboration), Phys. Lett. B **792**, 284 (2019).
[18] K. Morita, A. Ohnishi, F. Etminan, and T. Hatsuda, Phys. Rev. C **94**, 031901(R) (2016).
[19] K. Morita, S. Gongyo, T. Hatsuda, T. Hyodo, Y. Kamiya, and A. Ohnishi, arXiv:1908.05414v2.
[20] F. Wang, J. L. Ping, G. H. Wu, L. J. Teng, and T. Goldman, Phys. Rev. C **51**, 3411 (1995).
[21] H. R. Pang, J. L. Ping, F. Wang, T. Goldman, and E. G. Zhao, Phys. Rev. C **69**, 065207 (2004).
[22] M. Chen, H. X. Huang, J. L. Ping, and F. Wang, Phys. Rev. C **83**, 015202 (2011).
[23] H. X. Huang, J. L. Ping, and F. Wang, Phys. Rev. C **92**, 065202 (2015).
[24] Q. B. Li and P. N. Shen, Eur. Phys. J. A **8**, 417 (2000).
[25] Y. R. Liu and M. Oka, Phys. Rev. D **85**, 014015 (2012).
[26] W. Meguro, Y. R. Liu, and M. Oka, Phys. Lett. B **704**, 547 (2011).
[27] H. X. Huang, J. L. Ping, and F. Wang, Phys. Rev. C **87**, 034002 (2013).
[28] H. X. Huang, J. L. Ping, and F. Wang, Phys. Rev. C **89**, 035201 (2014).
[29] F. Fromel, B. Julia-Diaz, and D. O. Riska, Nucl. Phys. A **750**, 337 (2005).
[30] B. Julia-Diaz and D. O. Riska, Nucl. Phys. A **755**, 431 (2005).
[31] P. Junnarkar and N. Mathur, Phys. Rev. Lett. **123**, 162003 (2019).
[32] F. Wang, G. H. Wu, L. J. Teng, and T. Goldman, Phys. Rev. Lett. **69**, 2901 (1992); G. H. Wu, L. J. Teng, J. L. Ping, F. Wang, and T. Goldman, Phys. Rev. C **53**, 1161 (1996).
[33] H. X. Huang, P. Xu, J. L. Ping, and F. Wang, Phys. Rev. C **84**, 064001 (2011).
[34] J. L. Ping, F. Wang, and T. Goldman, Nucl. Phys. A **657**, 95 (1999); G. H. Wu, J. L. Ping, L. J. Teng *et al.*, *ibid.* **673**, 279 (2000); H. R. Pang, J. L. Ping, F. Wang, and T. Goldman, Phys. Rev. C **65**, 014003 (2001).
[35] L. Z. Chen, H. R. Pang, H. X. Huang, J. L. Ping, and F. Wang, Phys. Rev. C **76**, 014001 (2007).
[36] Y. Fujiwara, C. Nakamoto, and Y. Suzuki, Phys. Rev. Lett. **76**, 2242 (1996); Y. W. Yu, Z. Y. Zhang, P. N. Shen, and L. R. Dai, Phys. Rev. C **52**, 3393 (1995).
[37] A. Valcarce, H. Garcilazo, F. Fernández, and P. Gonzalez, Rep. Prog. Phys. **68**, 965 (2005), and references therein.
[38] J. Vijande, F. Fernandez, and A. Valcarce, J. Phys. G **31**, 481 (2005).
[39] C. Patrignani *et al.* (Particle Data Group), Chin. Phys. C **40**, 100001 (2016).
[40] M. M. Xu, M. Yu, and L. S. Liu, Phys. Rev. Lett. **100**, 092301 (2008).
[41] M. Kamimura, Supp. Prog. Theo. Phys. **62**, 236 (1977).
[42] V. A. Babenko and N. M. Petrov, Phys. At. Nucl. **66**, 1319 (2003).